

ANALYTICAL CONSIDERATIONS AND NUMERICAL SIMULATIONS FOR SURFACE PLASMON RESONANCE IN FOUR LAYERS PLASMONIC STRUCTURES WHICH CONTAIN HIGH REFRACTIVE INDEX WAVEGUIDE

Aurelian A. POPESCU¹, Laurențiu BASCHIR^{1C}, Dan SAVASTRU¹, Mihai STAFE^{2C}, Georgiana C. VASILE^{2C}, Sorin MICLOS¹, Constantin NEGUȚU²,
Mona MIHĂILESCU², Niculae N. PUȘCAS²

The Insulator-Metal-Insulator-Insulator (IMII) plasmonic structures present a great interest for the optical photonics devices. In this paper we present an analyze for coupling of light into plasmonic structures which contains a dielectric waveguide. We obtained the characteristic equation for the wave guides in the IMII structure by solving the Helmholtz equations in four homogeneous media. The characteristic equations for three and four layers have similar forms as established. Subsequently, the numerical simulations for TM waveguide modes and the coupling by a prism with the refractive index lower then waveguide were done. It was showed that, the TM0 mode is confined to the metal interface and can't be exited. Resonance coupling into higher waveguide modes may be realized for some film thicknesses.

Keywords: plasmonic waveguides, dispersion equation, amorphous chalcogenide films.

1. Introduction

Plasmonics forms a major part of the fascinating field of nanophotonics, which explores how electromagnetic fields can be confined over dimensions of the order of or smaller than the wavelength. It is based on interaction processes between electromagnetic radiation and conduction electrons at metallic interfaces, or in small metallic nanostructures, leading to an enhanced optical near field of sub-wavelength dimension. Research in this area demonstrates how a distinct and often unexpected behavior can occur if discontinuities or sub-wavelength structure is imposed. Another beauty of this field is that it is firmly grounded on classical physics. There is a very large interest for metal-insulator structures, because they support surface plasmon-polariton resonance which may confine the light near surface at shorter dimensions than the wavelength.

¹ National Institute R&D of Optoelectronics INOE 2000, 409 Atomistilor str., 077125, Magurele, Ilfov, Romania. E-mail: baschirlaurentiu@inoe.ro

² University POLITEHNICA of Bucharest, Physics Department, 313 Splaiul Independentei, 060042, Bucharest, Romania. E-mails: stafe@physics.pub.ro, georgiana.vasile@physics.pub.ro

The prism coupling [1] led very soon to the development of plasmonic sensors [2-4], the results being particularly impressive in the case of the biological selective sensors [5-7], the chalcogenide glasses being used for the determination of blood group and others type of sensors [6-9]. Fundamentals of plasmons can be acquired from Maier's book [10]. Davis [11] proposed the matrix method. The matrix method was used [12-14] by other to determine the resonance characteristics of four layer structure with finite thickness dielectric film by considering the metal film thick. Economou [15] and Burke et al. [16] derived and analyzed the dispersion relation for different multilayers structures with a special symmetry. Opolski [17] deals with investigations concerning numerical simulations of the plasmon resonances in optical planar structures without finding the analytical solutions. However this method can't calculate the electromagnetic field distribution in each layer.

The aim of our paper is to develop the characteristic equation in general form for the four-layer structure first. And second, drawing the appropriate numerical simulations for the structure comprising prism with low refractive index ($n = 1.51$) made from BK7 which may couple the light into higher refractive index ($n = 2.45$) films, As_2S_3 for instance. The structure make sense as allows the use of commercially available plates with 50 nm gold film designed for applications in plasmonic biosensors.

2. The dispersion equation for the simplest plasmon-polariton configuration

From the Maxwell's equations and assuming a harmonic time dependence of the form $\vec{E}(\vec{r}, t) = \vec{E}(\vec{r}) \cdot e^{-i\omega t}$ and homogeneous media, the Helmholtz type wave equation can be obtained for the electric field [8]:

$$\nabla^2 \vec{E}(\vec{r}, t) - \frac{\epsilon}{c^2} \cdot \frac{\partial^2 \vec{E}(\vec{r}, t)}{\partial t^2} = 0 \quad (1)$$

where $\epsilon(x) = n^2$ is the dielectric constant which depends only on x - spatial coordinate. For the magnetic field, the equation is similar.

Assuming the one-dimensional case and the waves propagating in the z direction [10] we can write the following wave equation for TE modes:

$$\frac{\partial^2 \vec{E}_y}{\partial x^2} + (k_0^2 \epsilon(z) - \beta^2) \vec{E}_y = 0 \quad (2)$$

where $k_0 = \omega/c$ is the wave vector of the propagating wave in vacuum. The complex parameter $\beta = k_z$ is called the propagation constant of the traveling

waves. The same equation can be written for the magnetic field. Being a vector equation, a system of 3 equations must be solved in general case.

The general analysis of the solutions of equation (2.2) is done in [18]. The concept consists in a definition of TM and TE modes in which the system may be reduced to one single differential equation. Then, the wave equation for TM modes will be:

$$\frac{\partial^2 \vec{H}_y}{\partial x^2} + (k_0^2 \varepsilon - \beta^2) \vec{H}_y = 0 \quad (3)$$

The simplest geometry which sustains surface plasmon polaritons (SPPs) is that of a single flat interface between a dielectric and a metal. Then, the solution of equation (2.3) leads to the dispersion equation which has the form:

$$\beta(\omega) = \frac{\omega}{c} \sqrt{\frac{\varepsilon_1 \cdot \varepsilon_2}{\varepsilon_1 + \varepsilon_2}} \quad (4)$$

Here, $\varepsilon_{1,2}$ are the dielectric constants of the adjacent media. To be mention that this is the only case when the dispersion equation $\beta(\omega)$ can be obtained in the explicit form [10], as $\varepsilon(\omega)$ are usually known values.

In practical cases which use the excitation of surface plasmons by attenuated total reflection¹, the three layers configuration which contains a thin metallic film is used. The dispersion equation corresponding to this case can be written in the form [10]:

$$e^{-4k_1 a} = \frac{k_1/\varepsilon_1 + k_2/\varepsilon_2}{k_1/\varepsilon_1 - k_2/\varepsilon_2} \cdot \frac{k_1/\varepsilon_1 + k_3/\varepsilon_3}{k_1/\varepsilon_1 - k_3/\varepsilon_3} \quad (5)$$

In Eq. 5 the metal film thickness is denoted $2a$ and k_i are the so called “transversal” wave vectors:

$$k_i = \sqrt{\beta^2 - k_0^2 \varepsilon_i}, \quad i = 1, 2, 3, 4. \quad (6)$$

A practical analysis of the Eq. (5) involves performing numerical calculations for modified equation named “characteristic equation” which can be deduced from eq. (5). Of course, once for the metal film ε is complex number, all k_i have to be imaginaries, too. The aim is to find the propagation constant $\beta = \beta_{real} + i\beta_{imaginary}$ whose real part describes the phase velocity and imaginary part describes the wave attenuation.

3. Four Layers Plasmonic Configuration - The Solution For The Electromagnetic Field

Multilayers structures have additional functionalities related to the confinement of the electromagnetic field. Among others, such structure provides

the coupling of light into planar waveguides structures that can support both TM and TE modes. The plasmonic waveguides contain at least one metallic medium which has a complex dielectric constant. As a result, the propagation waveguide constants are complex numbers. Finding the numerical solutions for the wave equation within these structures become more cumbersome so that finding of a suitable analytical form for the dispersion equation appears to be a necessity.

Fig. 1 presents a typical IMII (*insulator- metal- insulator/ chalcogenide -insulator*) structure. Layer '1' is a metallic film of thickness a , the layer '2' is the *chalcogenide* film of thickness d , whereas '3' and '4' are the semi-infinite dielectric media.

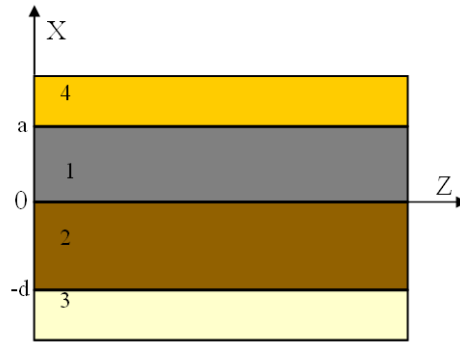


Fig. 1. Schematic picture of the 4-layers IMII structure that can support light confinement. The two finite thickness media have the thickness a (metal) and d (chalcogenide).

We will seek for the solutions of Eq. (3) as a sum of exponential functions for each medium which is considered homogeneous. By denoting the propagation constant with β , which is the same in all media due to the boundary conditions, the solutions of the wave equation for the TM modes (i.e. the magnetic H_y and electric E_z field components) can be written as follows:

$$H_y = Ae^{i\beta z} e^{-k_4 x} \quad \text{for } x > a, \quad (7)$$

$$E_z = iA \frac{1}{\omega \epsilon_0 \epsilon_4} k_4 e^{i\beta z} e^{-k_4 x} \quad \text{for } x > a, \quad (7)$$

$$H_y = Be^{i\beta z} e^{k_1 x} + Ce^{i\beta z} e^{-k_1 x} \quad \text{for } 0 < x < a, \quad (8)$$

$$E_z = -iB \frac{k_1}{\omega \epsilon_0 \epsilon_1} e^{i\beta z} e^{k_1 x} + iC \frac{k_1}{\omega \epsilon_0 \epsilon_1} e^{i\beta z} e^{-k_1 x}, \quad \text{for } 0 < x < a, \quad (8)$$

$$H_y = De^{i\beta z} e^{k_2 x} + Ee^{i\beta z} e^{-k_2 x} \quad (9)$$

$$E_z = -iD \frac{k_2}{\omega \epsilon_0 \epsilon_2} e^{i\beta z} e^{k_2 x} + iE \frac{k_2}{\omega \epsilon_0 \epsilon_2} e^{i\beta z} e^{-k_2 x}, \quad \text{for } -d < x < 0$$

$$H_y = Fe^{i\beta z} e^{k_3 x} \quad (10)$$

$$E_z = -iF \frac{1}{\omega \epsilon_0 \epsilon_3} k_3 e^{i\beta z} e^{k_3 x}, \quad \text{for } x < -d$$

3.1. Dispersion equation

Using the notation $r_i = k_i / \epsilon_i$, $r_{ij} = r_i / r_j$, $k_{ij} = k_i / k_j$ and taking in the account the continuity conditions for the TM modes we obtained the following equations:

$$\begin{aligned} Ae^{-k_4 a} &= Be^{k_1 a} + Ce^{-k_1 a} \\ Ar_4 e^{-k_4 a} &= -Br_1 e^{k_1 a} + Cr_1 e^{-k_1 a} \\ B + C &= D + E \\ -Br_1 + Cr_1 &= -Dr_2 + Er_2 \\ De^{-k_2 d} + Ee^{k_2 d} &= Fe^{-k_3 d} \\ -Dr_2 e^{-k_2 d} + Er_2 e^{k_2 d} &= -Fr_3 e^{-k_3 d} \end{aligned} \quad (11-16)$$

The system of six equations can be solved in general form using the determinants. However this way is rather voluminous. The following observations quickly lead to results. From Eqs. (11) and (12) one can obtain the ratio B/C . Similarly, from Eqs. (15) and (16) it results the ratio D/E :

From Eq. (13) it results E/C , whereas from Eq. (14) one can obtain E/C again.

The solution is obtained equating rightmost sides:

$$\left(\frac{1 + \frac{r_1 - r_4}{r_1 + r_4} e^{-2k_1 \cdot a}}{1 + \frac{r_2 + r_3}{r_2 - r_3} e^{2k_2 d}} \right) = \left(\frac{r_1}{r_2} \right) \cdot \left(\frac{1 - \frac{r_1 - r_4}{r_1 + r_4} e^{-2k_1 \cdot a}}{1 - \frac{r_2 + r_3}{r_2 - r_3} e^{2k_2 d}} \right) \quad (17)$$

For TE modes we simply replace r_i by k_i . In order to get the general case we introduce the next notations:

$$P = \begin{cases} \frac{\varepsilon_2}{\varepsilon_1} & \text{for TM} \\ 1 & \text{for TE} \end{cases}, \quad Q = \begin{cases} \frac{\varepsilon_2}{\varepsilon_3} & \text{for TM} \\ 1 & \text{for TE} \end{cases}, \quad R = \begin{cases} \frac{\varepsilon_2}{\varepsilon_4} & \text{for TM} \\ 1 & \text{for TE} \end{cases} \quad (18)$$

Eq. (17) becomes:

$$\left(\frac{1 + \frac{P \cdot k_1 - R \cdot k_4}{P \cdot k_1 + R \cdot k_4} e^{-2k_1 \cdot a}}{1 + \frac{k_2 + Q \cdot k_3}{k_2 - Q \cdot k_3} e^{2k_2 d}} \right) = \left(\frac{P \cdot k_1}{k_2} \right) \cdot \left(\frac{1 - \frac{P \cdot k_1 - R \cdot k_4}{P \cdot k_1 + R \cdot k_4} e^{-2k_1 \cdot a}}{1 - \frac{k_2 + Q \cdot k_3}{k_2 - Q \cdot k_3} e^{2k_2 d}} \right). \quad (19)$$

Terms containing $e^{2k_2 d}$ can be separated from those containing $e^{-2k_1 \cdot a}$. After separation it finally results:

$$e^{2k_2 d} = \left(\frac{k_2 + Q \cdot k_3}{k_2 - Q \cdot k_3} \right) \cdot \left(\frac{k_2 - P \cdot k_1}{k_2 + P \cdot k_1} \right) \cdot \left(\frac{1 + \frac{(k_2 + P \cdot k_1) \cdot (P \cdot k_1 - R \cdot k_4)}{(k_2 - P \cdot k_1) \cdot (P \cdot k_1 + R \cdot k_4)} e^{-2k_1 a}}{1 + \frac{(k_2 - P \cdot k_1) \cdot (P \cdot k_1 - R \cdot k_4)}{(k_2 + P \cdot k_1) \cdot (P \cdot k_1 + R \cdot k_4)} e^{-2k_1 a}} \right). \quad (20)$$

3.2 Fields distribution

We may find the amplitudes B-F of the magnetic/ electric fields within the IMII structure by applying boundary conditions and considering the amplitude of the incident field as unit ($A = 1$). Thus, for the TM modes we obtain:

$$H_y(x) = \begin{cases} e^{-k_4(x-a)} & x \geq a \\ \frac{1}{2} \left[(1 - r_{41}) e^{k_1(x-a)} + (1 + r_{41}) e^{-k_1(x-a)} \right] & 0 \leq x \leq a \\ \frac{\xi_{TM}}{2} \left[(1 - r_{32}) e^{-k_2(x+d)} + (1 + r_{32}) e^{k_2(x+d)} \right] & -d \leq x \leq 0 \\ \xi_{TM} e^{k_3(x+d)} & x \geq -d \end{cases} \quad (21)$$

$$\text{with } \xi_{TM} = \frac{(1 - r_{41}) e^{-k_1 a} + (1 + r_{41}) e^{k_1 a}}{(1 - r_{32}) e^{-k_2 d} + (1 + r_{32}) e^{k_2 d}}.$$

Similarly, for the TE-modes we obtain:

$$E_y(x) = \begin{cases} e^{-k_4(x-a)} & x \geq a \\ \frac{1}{2} \left[(1-r_{41})e^{k_1(x-a)} + (1+r_{41})e^{-k_1(x-a)} \right] & 0 \leq x \leq a \\ \frac{\xi_{TE}}{2} \left[(1-r_{32})e^{-k_2(x+d)} + (1+r_{32})e^{k_2(x+d)} \right] & -d \leq x \leq 0 \\ \xi_{TE} e^{k_3(x+d)} & x \geq -d \end{cases} \quad (22)$$

$$\text{with } \xi_{TE} = \frac{(1-k_{41})e^{-k_1 a} + (1+k_{41})e^{k_1 a}}{(1-k_{32})e^{-k_2 d} + (1+k_{32})e^{k_2 d}}$$

Since k_i appearing in these relations are functions of propagation constants β (see eq. (6)), we must first solve numerically the dispersion equation.

3.3. Characteristic equation

In order to obtain a more suitable form for numerical calculations of the propagation constant, we may take into account that k_2 and r_2 are complex quantities. A good idea is therefore to replace k_2 and r_2 with imaginary ones: $k_2 = i \cdot \bar{k}_2$ and $r_2 = i \cdot \bar{r}_2$. Taking into account that:

$$e^{2k_2 d} = e^{2i \cdot \bar{k}_2 d} = \frac{\cos(\bar{k}_2 d) + i \cdot \sin(\bar{k}_2 d)}{\cos(\bar{k}_2 d) - i \cdot \sin(\bar{k}_2 d)} = \frac{1 + i \cdot \tan(\bar{k}_2 d)}{1 - i \cdot \tan(\bar{k}_2 d)} = \frac{1 + i \cdot t}{1 - i \cdot t} \quad (23)$$

where $t = \tan(\bar{k}_2 \cdot d)$, and denoting $s = \frac{P \cdot k_1 - R \cdot k_4}{P \cdot k_1 + R \cdot k_4} e^{-2k_1 a}$ and $g = \frac{Q \cdot k_3}{\bar{k}_2}$, eq.

(19) becomes:

$$\left(\frac{1+s}{1 + \left(\frac{1-i \cdot g}{1+i \cdot g} \right) \cdot \left(\frac{1+i \cdot t}{1-i \cdot t} \right)} \right) = \left(\frac{P \cdot k_1}{i \cdot \bar{k}_2} \right) \cdot \left(\frac{1-s}{1 - \left(\frac{1-i \cdot g}{1+i \cdot g} \right) \cdot \left(\frac{1+i \cdot t}{1-i \cdot t} \right)} \right), \quad (24)$$

with $f = \left(\frac{P \cdot k_1}{\bar{k}_2} \right) \frac{1-s}{1+s}$ and $u = \frac{t-g}{1+tg}$. Eq. (24) can be written as:

$$\frac{i}{1 + \frac{1+i \cdot u}{1-i \cdot u}} = \frac{f}{1 - \frac{1+i \cdot u}{1-i \cdot u}} \quad (25)$$

where is easily seen that $f = u$. This means that $f = \frac{t-g}{1+tg}$ and therefore $t = \tan(\bar{k}_2 \cdot d) = \frac{f+g}{1-fg}$. Finally, the characteristic equation can be written as follow:

$$d = \frac{\arctan(f) + \arctan(g) + m \cdot \pi}{\bar{k}_2} \quad (26)$$

The characteristic equations for the four-layer structure have the same form as the equation obtained earlier by Marcuse¹⁹ for the three-layer lossless structure. The difference consists of more general value for the coefficients f and g . The simulations have been done in the field of complex numbers. Some practical remarks are considered:

First: we normalized all the parameters dividing or multiplying them to $k_0 = 2\pi/\lambda$. We obtained $B = (\beta/k_0)^2$, $\alpha = k_0 a$ and $\delta = k_0 d$. Also, we introduced the following notations:

$$\begin{aligned} u_1 &= \sqrt{B - \varepsilon_1} \\ u_2 &= \sqrt{\varepsilon_2 - B} \\ u_3 &= \sqrt{B - \varepsilon_3} \\ u_4 &= \sqrt{B - \varepsilon_4} \end{aligned} \quad (27)$$

Eq. (26) becomes:

$$\delta = \frac{\arctan(f) + \arctan(g) + m \cdot \pi}{u_2} \quad (28)$$

where f and g can be determined as:

$$f = \left(\frac{P \cdot u_1}{u_2} \right) \frac{1-s}{1+s} \text{ and } g = \frac{Q \cdot u_3}{u_2}, \text{ with } s = \frac{P \cdot u_1 - R \cdot u_4}{P \cdot u_1 + R \cdot u_4} e^{-2u_1\alpha}.$$

Second: solving Eq. (28) means finding zeroes of a complex function. This can be achieved by using Newton algorithm, for instance. Attention should be paid to the sense of the iterative process because, at large values of d , $\sqrt{B} = \beta/k_0$ has a horizontal asymptote and the algorithm will fail. Also, the starting guess for B should be a complex value, even if the imaginary part is very small. Else the algorithm will work only in the real domain, rather finding complex solutions.

4. Numerical simulations for the 4 layer plasmonic structure with As_2S_3 waveguide

The characteristic equation (26) was solved numerically in MATLAB to find the propagation constant. The propagation constant was inserted in eq. (6) to calculate k_i and, subsequently, the electric and magnetic fields of the TM and TE modes. The incident laser wavelength is 632.8 nm and the four layers of the IMII structure are as follows (see Fig. 1): layer 4-BK7, layer -Au, layer 2- As_2S_3 and layer 3-Air. The thickness of the Au film is considered $a = 50 \text{ nm}$ and the chalcogenide film thickness (d) is varied between 200 and 1600 nm. In our simulations we consider for chalcogenide film $n_2 = 2.45$. The gold optical constant is taken from Rakic [20]. We find for the wavelength 632.8 nm the following refractive index value: $N = 0.196 - i3.256$.

First, let us present the results regarding the TM modes. The real part of the effective refractive index $N_{\text{eff}} = \beta/k_0$ as a function of chalcogenide film thickness d for the TM modes is presented in Fig. 2a.

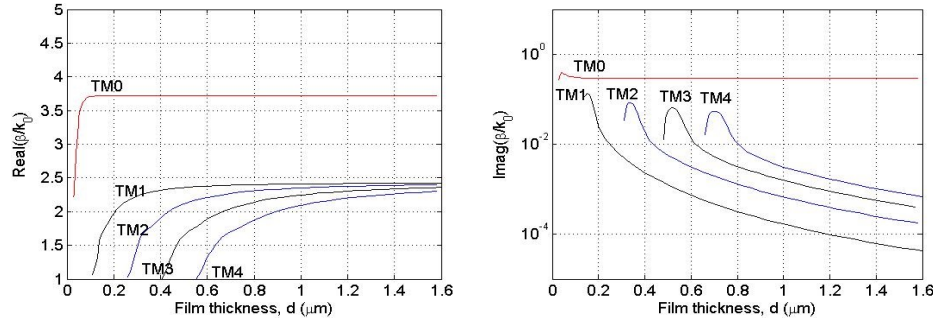


Fig. 2. The real part (a) and imaginary part (b) of the propagation constant for the TM modes. The simulation parameters were: $a = 50 \text{ nm}$, $\lambda = 632.8 \text{ nm}$.

In the prism, the wave vector component parallel to the interface is $(k_0 n_p \sin \theta)$ and must be equal to propagation constant β . The maximum value is obtained for $\theta = 90^\circ$, where θ is the angle of incidence and $n_p = 1.51$. The effective refractive index of the multilayer structure is contained in the range [1, 1.51] for some As_2S_3 film thicknesses and depends on the mode number. The higher values of the effective refractive indices could not really be excited due to synchronization conditions. The resonant angle θ corresponds to the condition: $n_p \sin \theta = N_{\text{eff}}$.

The following conclusions can be drawn proceeding from Fig. 2: a) the mode TM0 never can be excited with a prism made from BK7 glass as the effective refractive index always is higher than two. b) For each, special selected thickness, only one mode can be coupled. For example, for the film thickness of 600 nm, only the TM4 mode can be coupled. c) the TM0 mode has the highest attenuation coefficient. Fig. 3 presents the magnetic field within the four regions of the structure for different TM modes, calculated using the above presented formula.

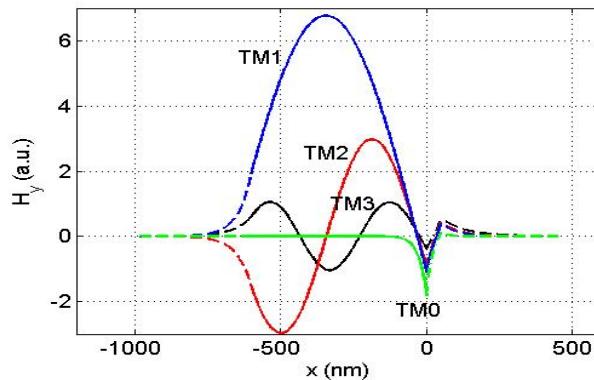


Fig. 3. The magnetic field distribution within the structure for different TM modes. The simulation parameters are: $d = 600$ nm, $a = 50$ nm, $\lambda = 632.8$ nm.

The light intensity distributions within layers are presented in Fig. 4.

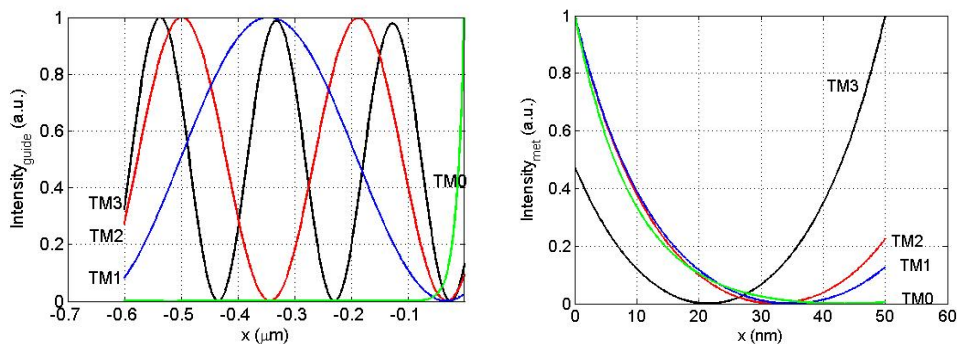


Fig. 4. The light intensity distribution within the As₂S₃ waveguide (left) and within the metal film (right). The value $x=0$ corresponds to the metal-chalcogenide film interface.

6. Conclusions

The characteristic equation for the case of four layers plasmonic structure was derived by solving the equations for the electromagnetic field. The characteristic equation is similar to the one designed for the three layers configuration, the difference being only in the form of the involved parameters. By solving numerically the characteristic equation we determined the effective refractive index (β/k_0), attenuation and field distributions as a function of chalcogenide film thickness for BK7-Au-As₂S₃-Air IMII plasmonic structure. The four layers structure becomes similar to three layers MII structure when increasing the metallic layer thickness above 100 nm.

The plasmonic structure containing a finite thick metal film and a finite thick dielectric film supports several waveguides modes. For some well-defined thicknesses, the light can be coupled into plasmonic waveguide modes from a BK7 prism ($n = 1.51$) with the refractive index lower than the refractive index of As₂S₃ chalcogenide film ($n = 2.45$). The practical significance of provided analyze is represented by the possibility of using commercially glass slides with already deposited gold film. The attractivity of using chalcogenide As₂S₃ amorphous films is that they are light sensitive optical material which supports photoinduced changes of the refractive index. The structure presents a high interest for the development of the optical switches, 2D memories or sensing elements that use optical active materials such as amorphous chalcogenides.

Acknowledgments

The financial support offered by a grant of the Romanian National Authority for Scientific Research, CNDI – UEFISCDI, project number PN-II-PT-PCCA-2011- 25/2012 is kindly acknowledged.

R E F E R E N C E S

- [1] *Kretschmann E., and Raether, H.*, “Radiative decay of non-radiative surface plasmons excited by light”, *Z. Naturforschung*, **23A**: (1968), pp.2135–2136.
- [2] *Homola J., Sinclair S. Yee, Gunter Gauglitz*, “Surface plasmon resonance sensors: review”, *Sensors and Actuators B* **54**, (1999), pp.3-15.
- [3] *Berini Pierre*, “Plasmon-polariton modes guided by a metal film of finite width bounded by different dielectrics”, *Optics Express* Vol. **7**(10), (2000), pp.329-335.
- [4] *Gauvreau Bertrand, Hassani Alireza, Fehri Majid Fassi, Kabashin Andrei, Skorobogatiy Maksim*, “Photonic bandgap fiber-based Surface Plasmon Resonance sensors”, *Optics Express* Vol. **15**(18), (2007), pp.11413-11426
- [5] *Hoaa X.D., Kirk A.G., Tabrizian M.*, “Towards integrated and sensitive surface plasmon resonance biosensors: A review of recent progress”, *Biosensors and Bioelectronics* **23**, (2007), pp.151-160

- [6] *Sharma Anuj K., Jha Rajan, Pattanaik Himansu S.* “Design considerations for surface plasmon resonance based detection of human blood group in near infrared”, *J. Appl. Phys.* **107**, (2010), article number 034701.
- [7] *Rajan Jhaa, Anuj K. Sharmab*, “Design of silicon based plasmonic biosensor chip for human blood group detection”, *Sensors and Actuators B* **145**, (2010), pp.200-204.
- [8] *Charnovych S., Szabo I.A., Toth A.L., Volk J., Trunov M.L., Kokenyesi S.*, “Plasmon assisted photoinduced surface changes in amorphous chalcogenide layer”, *J. Non-Cryst. Solids*, Vol. **377**(SI), (2013), pp.200-204.
- [9] *Sámson Zsolt L., Yen Shih-Chiang, MacDonald Kevin F., Knight Kenton, Li Shufeng, Hewak Daniel W., Tsai Din-Ping, and Zheludev Nikolay I.*, “Chalcogenide glasses in active plasmonics”, *Phys. Status Solidi RRL*, Vol. **4**(10), (2010), pp.274–276.
- [10] *Maier S. A.*, [Plasmonics: Fundamentals and Applications,] Springer, 2007.
- [11] *Davis T.J.*, “Surface plasmon modes in multi-layer thin-films”, *Opt. Commun.* **282**, (2009), pp.135-140.
- [12] *Popescu A.A., Savastru R., Savastru D., Miclos S.*, “Application of vitreous As-S-Se chalcogenides as active layer in surface plasmon resonance configuration”, *Dig. J. Nanomater. Biostuct.* Vol **6**(3), (2011), pp.1245-1252.
- [13] *Vasile Georgiana C., Savastru Roxana, Popescu A. A., Stafe M., Savastru D., Dontu Simona, Baschir L., Sava V., Chiricuța B., Mihailescu M., Negutu C., and Puscas N. N.*, “Modelling the 2D plasmonic structures with active chalcogenide glass layer”, *Rom. Rep. Phys.* Vol. **65**(3), 1012-1018 (2013).
- [14] *Vasile Georgiana C., Popescu Aurelian A., Stafe Mihai, Koziukhin S.A., Savastru Dan, Dontu Simona, Baschir L., Sava V., Chiricuță B., Mihailescu Mona, Neguțu Constantin, Puscas Niculae N.*, “Plasmonic waveguides features correlated with surface plasmon resonance performed with a low refractive index prism,” *U.P.B. Sci. Bull. Series A* Vol. **75**(4), (2013), pp. 311-325.
- [15] *Economou E. N.*, “Surface plasmons in thin films”, *Phys. Rev. E* **182** (8), (1969), pp. 539-554.
- [16] *Burke J.J., Stegeman G.I., Tamir T.*, “Surface-polariton-like waves guided by thin, lossy metal film”, *Phys. Rev. B*, **33** (8), (1986), pp. 5186-5201.
- [17] *Opilski Z.*, “Analysis of Surface Plasmons in the Optical Planar Waveguide with Spectral Detection”, *Acta Physica Polonica*, Vol. **118** (6), (2010), pp.1209-1214.
- [18] *Yariv A.*, Book [Optical electronics in modern communications] 5th ed., Oxford University Press, New York, 1997.
- [19] *Marcuse D.*, Book [Theory of Dielectric Optical Waveguides,] New York: Academic Press, 1974.
- [20] *Rakić A. D., Djurišić A. B., Elazar J. M., and Majewski M. L.*, “Optical properties of metallic films for vertical-cavity optoelectronic devices,” *Appl. Opt.* **37**, (1998), pp. 5271-5283.